9

Energy efficiency of Fuel Processor – PEM Fuel Cell systems

Lucia Salemme, Laura Menna and Marino Simeone
University of Naples "Federico II", Department of Chemical Engineering
Italy

1. Introduction

As the world moved into the 21st century, a rapid development in industrial and transportation sectors and improvements in living standards have been observed, leading to a strong growth in the energy demand and in global emissions (Song, 2002). In this context, fuel cell technology has been receiving an increasing attention, thanks to its lower emissions and potentially higher energy efficiency if compared with internal combustion engines. A fuel cell is defined as an electrochemical device in which the chemical energy stored in a fuel is converted directly into electricity. Among all fuel cells, low temperature Proton Exchange Membrane Fuel Cells (PEMFC) are promising devices for decentralized energy production, both in stationary and automotive field, thanks to high compactness, low weight (high power-to-weight ratio), high modularity and efficiency, fast start-up and response to load changes.

The ideal fuel for PEMFC is hydrogen with low carbon monoxide content to avoid poisoning of the fuel cell; in this way, PEMFC can achieve efficiency up to 60%, far higher if compared to 20-35% efficiency of an internal combustion engine.

Hydrogen, though, is not a primary source. It is substantially an energy carrier, that can be stored, transported and used as gaseous fuel, but, it needs to be produced from other fuels.

Today most of the hydrogen produced is obtained by hydrocarbons in large industrial plants through the well-known Steam Reforming and Autothermal Reforming processes.

However, hydrogen distribution from industrial production plants to small-scale users meets some limitations related to difficulties in hydrogen storage and transport. For its chemical and physical properties, indeed, the development of an hydrogen infrastructure seems to be not feasible in short term, while more reasonable seems to be the concept of decentralized hydrogen production; in this way, an hydrogen source, such as methane, is distributed through pipelines to the small-scale plant, placed nearby users, and the *in situ* produced hydrogen is fed directly to the energy production system, avoiding hydrogen storage and transportation. In this sense, a compact fuel processor, capable of generating a hydrogen rich stream from an easily transportable fuel, is a potential root to accelerate PEMFC deployment in the near future.

A typical fuel processor is constituted by a reforming unit coupled with a CO clean-up section, introduced to guarantee hydrogen production with a CO content compatible with

PEMFC specifics. In particular, two different kinds of fuel processor are most frequently described in the scientific literature; a conventional one, in which the reforming unit is followed by two water gas shift (WGS) reactors and a preferential CO oxidation (PROX) reactor (Ersoz et al, 2006), and an innovative one, in which the reforming unit is coupled with highly selective hydrogen membranes to produce pure hydrogen, allowing to operate the PEMFC without a purge stream, generally named as anode off-gas (Lattner et al, 2004).
The global energy efficiency of these systems strictly depends on fuel processor configuration and on operating conditions; therefore, a comprehensive simulative analysis of fuel processors coupled with a PEMFC can contribute to identify the conditions that maximize system performance.
The following paragraphs provide a detailed description of conventional and membrane-based fuel processors. In particular, section 2.1 describes the conventional fuel processors, with details on the reforming technologies and on the typical CO clean-up techniques, while section 2.2 describes innovative fuel processor and membrane technology. Section 2.3 reviews the state of art of the analysis of fuel processor – PEMFC system. Section 3 and 4 report the methodology employed to simulate system performance and the results obtained, respectively. Finally, section 5 draws the main conclusions on the energy efficiency analysis presented.

2. Fuel Processor - PEMFC systems

2.1 Conventional Fuel Processors

Fig. 1 shows the scheme of a conventional fuel processor for hydrogen production from methane, which consists of a desulfurization unit (Des), a syngas production section and a CO clean-up section.

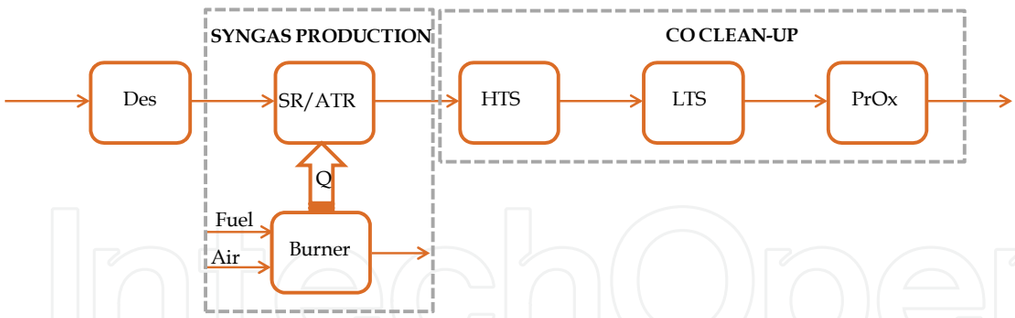

Fig. 1. Conventional Fuel Processor

The desulfurization section is required to lower the sulfur content of the fuel to 0.2 ppm, both for environmental and catalysts restrictions; it generally consists of an hydrodesulphurization reactor, where hydrogen added to the fuel reacts with the sulfur compounds to form H_2S, followed by an adsorption bed to remove H_2S.
The desulfurization process is a quite mature technology and its optimization is essentially related to the catalytic system and it will not be analyzed further. A comprehensive treatment of this unit can be found in Lampert et al, 2004.
The syngas production section is generally used to convert the fuel into syngas, a mixture of H_2 and CO. Two main syngas production technologies are generally employed: Steam

Reforming and Autothermal Reforming. The thermodynamic analysis of reforming processes is widely discussed in the literature (Seo et al, 2002), as well as the optimization of catalyst formulation and operating conditions that maximize process performance (Xu et al, 2006, Semelsberger et al, 2004).

The Steam Reforming process is realized by feeding methane and steam to a catalytic reactor, where the following reactions take place:

1) $CH_4 + H_2O = CO + 3H_2$ $\Delta H^o_R = 49$ Kcal/mol CH_4

2) $CO + H_2O = CO_2 + H_2$ $\Delta H^o_R = -9.8$ Kcal/mol CO

3) $CH_4 = C + 2H_2$ $\Delta H^o_R = 18$ Kcal/ mol CH_4

The operative parameters that influence this process are: pressure (P), temperature (T_{SR}) and steam to methane ratio (H_2O/CH_4) in the feed.

By observing reactions 1, 2 and 3, the reader will be easily convinced that the process occurs with an increment of number of moles; therefore it is favored by low pressures.

The process is globally endothermic and it is favored by high temperatures. The heat required for the reaction is supplied by an external burner fed with additional fuel and air.

Usually, reactor temperature does not exceed 800°C ca. due to catalyst and construction materials constraints.

The value of H_2O/CH_4 employed is usually higher than 2 (stoichiometric value), to reduce coke formation and lower than 4, to limit operative cost and reactor size.

Due to its high selectivity and to the high concentration of hydrogen in the product stream, steam reforming is the most common process to produce hydrogen from hydrocarbons.

However, when looked at from a "decentralized hydrogen production" perspective, it shows some disadvantages essentially because of reduced compactness and slow response to load changes. Both aspects should be attributed to the endothermicity of the reaction and to the high residence times required.

Auto thermal Reforming is obtained by adding air to the inlet SR mixture; in this way, the heat for the endothermic reforming reactions is supplied by the oxidation of part of the methane inside the reactor itself.

The amount of air must be such that the energy generated by the oxidation reactions balances the energy requirement of the reforming reaction, maintaining reactor temperature to typical SR values (600-800°C).

The internal heat generation offers advantages in terms of reactor size and start up times; however, the addition of air to the feed lowers hydrogen concentration in the reformate stream due to the presence of large amounts of nitrogen, fed to the reactor as air.

Either through Steam reforming or Autothermal reforming, the outlet of the reactor has potential of further hydrogen production. Indeed, being reaction 2 exothermic, it is limited by the high temperatures typical of the reforming reactor. For this reason, another reaction step usually follows the main reforming reactor and reduces CO content to less than 10 ppm. This CO clean-up section is constituted by two water gas shift (WGS) reactors and a preferential CO oxidation (PROX) reactor.

The WGS process is a well-known technology, where the following reaction takes place:

4) $CO + H_2O = CO_2 + H_2$ $\Delta H°_R = -9.8$ Kcal/mol CO

WGS is realized in two stages with inter-cooling; the first stage is generally operated at 350-420°C and is referred to as "high temperature stage" (HTS), whereas the second stage is operated at 200-220°C and is referred to as "low temperature stage" (LTS). The outlet CO concentration from LTS is 0.2 - 0.5% ca. and a further CO conversion stage must be present

before the mixture can be fed to a PEMFC. In conventional fuel processors, CO is reduced to less than 50 ppm in a preferential CO Oxidation (PrOx) stage. The reactor is generally adiabatic and catalyst as well as operating conditions must be carefully chosen, in order to promote CO conversion whilst keeping hydrogen oxidation limited. This CO purification technology is mature and well defined, although it has disadvantage in terms of compactness and catalyst deactivation.
The stream leaving the fuel processor is generally named as reformate and contains the hydrogen produced, as well as CO_2, H_2O, unreacted CH_4 and N_2. This stream is ready to be sent to a PEMFC.

2.2 Innovative Fuel Processors

Innovative Fuel Processors are characterized by the employment of a membrane reactor, in which a high selective hydrogen separation membrane is coupled with a catalytic reactor to produce pure hydrogen.
A typical membrane reactor is constituted by two co-axial tubes, with the internal one being the hydrogen separation membrane; generally, the reaction happens in the annulus and the permeate hydrogen flows in the inner tube.
The stream leaving the reaction is named retentate and the stream permeated through the membrane is named permeate.
Membrane reactor is illustrated in Fig. 2 for the following generic reaction:
$A + B = C + H_2$
The membrane continuously removes the H_2 produced in the reaction zone, thus shifting the chemical equilibrium towards the products; this allows obtaining higher conversions of reactants to hydrogen with respect to a conventional reactor, working in the same operating conditions.
A typical membrane used to separate hydrogen from a gas mixture is a Palladium or a Palladium alloy membrane (Shu et al., 1991); this kind of membrane is able to separate hydrogen with selectivity close to 100%. Hydrogen permeation through Palladium membranes happens according to a solution/diffusion mechanism and the hydrogen flux through the membrane, J_{H2} is described by the following law:

$$J_{H2} = \frac{\mu_{H2} A}{\delta}\left(\sqrt{P_{H2,R}} - \sqrt{P_{H2,P}}\right) \quad (1)$$

where μ_{H2} is the permeability coefficient [mol/(m² s $Pa^{0.5}$)], A is the membrane surface area [m²], δ is the membrane thickness [m] and $P_{H2,R}$ and $P_{H2,P}$ are hydrogen partial pressures [kPa] on the retentate side and on the permeate side of the membrane, respectively. Eq. 1 is known as Sievert's law and it is valid if the bulk phase diffusion of atomic hydrogen is the rate limiting step in the hydrogen permeation process.
To increase the separation driving force, usually the retentate is kept at higher pressure than the permeate. In common applications, permeate pressure is atmospheric and retentate pressure is in the range 10-15 atm (compatibly with mechanical constraints).
A possible way to further increase the separation driving force is to reduce hydrogen partial pressure in the permeate ($P_{H2,P}$) by diluting the permeate stream with sweep gas (usually superheated steam).

Sievert's law shows that an increase of the hydrogen flux is achieved with reducing membrane thickness. Palladium membranes should not be far thinner than 80-100 µm due to mechanical stability of the layer and to the presence of defects and pinholes that reduce hydrogen selectivity. To overcome this problem, current technologies foresee a thin layer (20-50 µm) of Pd deposited on a porous ceramic or metal substrate.
Another important issue of Pd membranes (pure or supported) is thermal resistance. Temperature should not be less than 200°C, to prevent hydrogen embrittlement and not higher than 600°C ca. to prevent material damage.

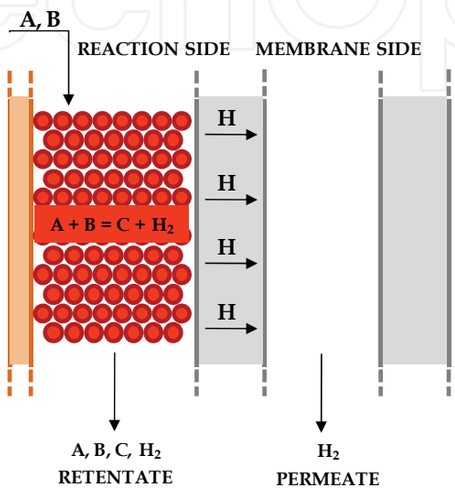

Fig. 2. Membrane Reactor

Innovative fuel processors can be realized by combining the membrane either with the reforming unit, generating the fuel processor reported in Fig. 3 (FP.1), or with a water gas shift unit, generating the fuel processor reported in Fig. 3 (FP.2).

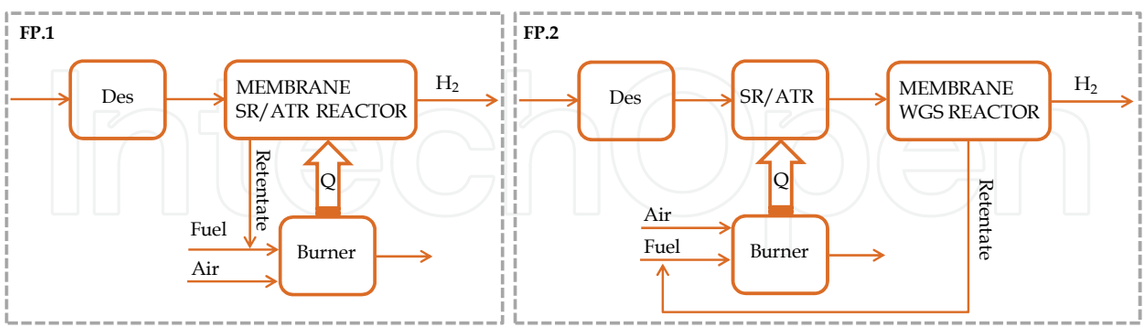

Fig. 3. Innovative Fuel Processors

FP.1 consists of a desulfurization unit followed by a membrane reforming reactor, with a burner. This solution guarantees the highest compactness in terms of number of units, since it allows to totally suppress the CO clean-up section; indeed, when the membrane is integrated in the reforming reactor, the permeate stream is pure hydrogen, that can be directly fed to a PEMFC.

However, this solution limits the choice of the operating temperature of the process that must be compatible with the constraints imposed by the presence of a membrane.
FP.2 consists of a desulfurization unit followed by a reforming reactor and a membrane water gas shift reactor. In this case, the membrane is placed in the low temperature zone of the fuel processor, operating at thermal levels compatible with its stability. This solution, although less compact than the previous one, allows to operate the syngas production section at higher temperature.

2.3 PEMFC

A fuel cell is an electrochemical device that converts the chemical energy of a fuel directly into electrical energy. Intermediate conversions of the fuel to thermal and mechanical energy are not required. All fuel cells consist of two electrodes (anode and cathode) and an electrolyte.
Proton exchange membrane fuel cells, also known as polymer electrolyte membrane fuel cells (PEMFC), are a type of fuel cell in which the electrolyte is a polymeric membrane and the electrodes are made of platinum.
In a PEMFC unit, hydrogen is supplied at one side of the membrane where it is split into hydrogen protons and electrons, at anode electrode:

$H_2 \rightarrow 2H^+ + 2e^-$

The protons permeate through the polymeric membrane to the reach the cathode electrode, where oxygen is supplied and the following reactions takes place.

$O_2 + 4H^+ + 4e^- \rightarrow 2H_2O$

Electrons circulate in an external electric circuit under a potential difference.
The electric potential generated in a single unit is about 0.9V. To achieve a higher voltage, several membrane units need to be connected in series, forming a fuel cell stack. The electrical power output of the fuel cell is about 60% of its energy generation, the remaining energy is released as heat.
Generally, oxygen is fed to the cathode as an air stream; in practical systems, an excess of oxygen is fed to the cathode to avoid extremely low concentration at the exit. Frequently, a 50% or higher excess with respect to the stoichiometric oxygen is fed to the cathode.
For the anode, instead, it is not typically the stoichiometric ratio, but rather the amount of hydrogen converted to the fuel cell as a percentage of the feed that is specified. This amount is named as the hydrogen utilization factor U_f; when pure hydrogen is fed to the PEMFC, this factor can be assumed equal to unity.
For PEMFC systems running on reformate produced in a conventional fuel processor, this factor can be assumed equal to 0.8. This implies that not all gas fed to the anode is converted and unconverted hydrogen and the rest of the reformate is purged off as a stream named as Anode Off-Gas (AOG). This stream presents a heating value due to the presence of hydrogen and methane; therefore, it can be used in the burner of the conventional fuel processor to eventually supply heat to the process.

2.4 System Analysis of Fuel Processor - PEMFC systems

Optimization of energy efficiency of a fuel processor PEMFC system is a central issue in actual research studies. Since the efficiency of the PEMFC can be assumed as a constant

equal to 60%, the efficiency of the entire system depends on fuel processor efficiency and on the integration between the fuel processor and the PEMFC.
The optimization of system efficiency is achieved by exploring the effect of the operating parameters considering, at the same time, the heat recovery between the various streams and units present in the system and the necessary driving force for heat exchange.
The optimization of conventional hydrocarbon-based fuel processors has been tackled by several authors who have identified the most favorable operating conditions to maximize the reforming efficiency. As a general outcome, SR-based fuel processors provide the highest hydrogen concentration in the product stream, whereas the highest reforming efficiency is reached with ATR-based fuel processors, due to the energy loss represented by the latent heat of vaporization of the water that escapes with the combustion products in the SR system (Ahmed et al, 2001).
However, as the system grows in complexity, due to the presence of the fuel cell, optimization of the global energy efficiency must also take into account the recovery of the energy contained in the spent gas released at the cell anode (anode off-gas). Ersoz et al. (2006) performed an analysis of global energy efficiency on a fuel processor – PEMFC system, considering methane as the fuel and steam reforming, partial oxidation and auto thermal reforming as alternative processes to produce hydrogen. Their main conclusion is that the highest global energy efficiency is reached when SR is used, essentially due to the higher recovery of anode off-gas heating value.
As far as membrane-based fuel processor is concerned, only few contributions which address the behavior of the entire system are available, that include not only the membrane-based fuel processor, but also the fuel cell, the auxiliary power units and the heat exchangers (Pearlman et al, Lattner et al, Manzolini et al, Campanari et al, Lyubovsky et al). Most of these studies refer to liquid fuels and only few contributions are available when methane is employed.
In particular, Campanari et al. (2008) analyzed an integrated membrane SR reactor coupled with a PEMFC, showing that a higher global energy efficiency can be achieved, with respect to conventional fuel processors, if a membrane reactor is employed.
Lyubovsky et al. (2006) analyzed a methane ATR-based fuel processor – PEMFC system, with a membrane unit placed downstream the WGS unit and operating at high pressure, concluding that high global energy efficiency can be obtained if a turbine is introduced in the system to generate additional power from the expansion of the hot gases produced by the combustion of the membrane retentate stream.
In order to have a complete vision of the effect of system configuration and of operating parameters on the efficiency of fuel processor – PEMFC systems, a comprehensive analysis of different configurations will be presented and compared in terms of energy efficiency; in particular, methane will be considered as fuel and SR and ATR as reforming processes; the focus of the discussion will be about the following fuel processor (FP) configurations, each coupled with a PEMFC:
FP.A) SR reactor, followed by two WGS reactors and a PROX reactor.
FP.B) ATR reactor, followed by two WGS reactors and a PROX reactor.
FP.C) Integrated membrane-SR reactor.
FP.D) Integrated membrane-ATR reactor.
FP.E) SR reactor followed by a membrane WGS reactor.
FP.F) ATR reactor followed by a membrane WGS reactor.

Each system configuration is investigated by varying operating parameters, such as steam to methane and oxygen to methane inlet ratios, reforming temperature, as well as pressure; the effect of the addition of steam as sweep gas on the permeate side of the membrane reactors will be also presented and discussed.

3. Methodology

The simulations were performed in stationary conditions, by using the commercial package Aspen Plus®. The selected property method was Peng-Robinson and the component list was restricted to CH_4, O_2, N_2, H_2O, CO, H_2 and CO_2.
Methane was considered as fuel, fed at 25°C and 1 atm, with a constant flow rate of 1 kmol/h. Feed to the system was completed with a liquid water stream (25°C and 1 atm) both in SR and ATR-based FPs; an air stream (25°C and 1 atm) is also present in the ATR-based FPs.
The configurations simulated (flow sheets) are presented in the following sections, where the assumptions and the model libraries used to simulate the process are presented. Section 3.1 is dedicated to conventional fuel processors, whereas membrane-based fuel processors are described in section 3.2. The quantities employed to calculate energy efficiency are defined in section 3.4.

3.1 Conventional fuel processor – PEMFC systems

Fig. 4 reports the flow sheet of a conventional SR-based fuel processor coupled with a PEMFC (FP.A). The fuel processor consists of a reforming and a CO clean-up section.

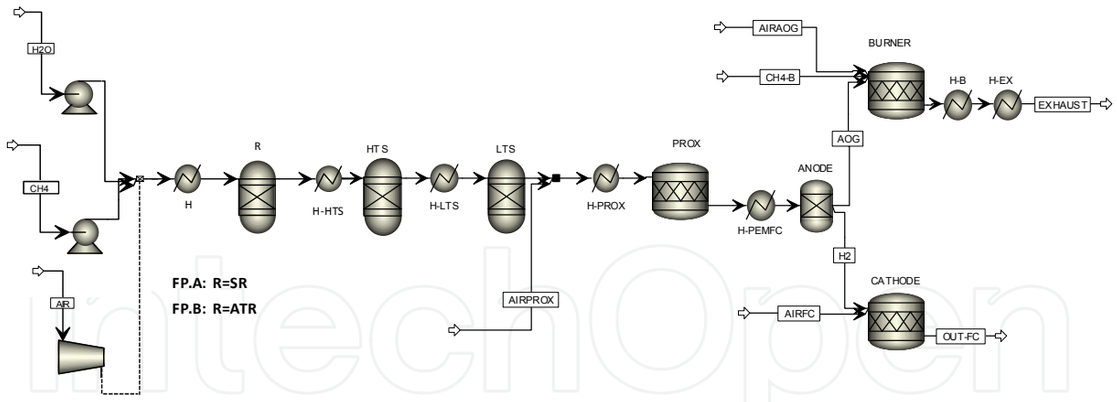

Fig. 4. Flowsheet of fuel processor FP.A and FP.B coupled with a PEMFC

The reforming section is an isothermal reactor (SR), modeled by using the model library ***RGIBBS.***
The CO clean-up section consists of a high (HTS) and low (LTS) temperature water gas shift reactor followed by a PROX reactor. HTS and LTS were modeled by using model library ***RGIBBS***; the reactors were considered as adiabatic and methane was considered as an inert in order to eliminate the undesired methanation reaction, kinetically suppressed on a real catalytic system.

The inlet temperature to the HTS reactor was fixed at 350°C, while the inlet temperature to the LTS one at 200°C. The PROX reactor was modeled as an adiabatic stoichiometric reactor, ***RSTOIC***; this kind of reactor models a stoichiometric reactor with specified reaction extent or conversion; in the case of PROX, two reactions were considered: oxidation of CO to CO_2 with complete conversion of CO and oxidation of H_2 to H_2O; the air fed to the PROX reactor (AIR-PROX) was calculated in order to achieve a 50% oxygen excess with respect to the stoichiometric amount required to convert all the CO to CO_2. The ***RSTOIC*** specifics were completed with the assignment of total conversion of CO and O_2. The inlet temperature to the PROX reactor was fixed at 90°C.
The PEM fuel cell section is simulated as the sequence of the anode, modeled as an ideal separator, ***SEP***, and the cathode, modeled as an isothermal stoichiometric reactor, ***RSTOIC.*** The presence of the ***SEP*** unit allows to model a purge gas (anode off-gas, AOG) required for mass balance reasons, whenever the hydrogen stream sent to the PEM fuel cell is not 100% pure. In agreement with the literature, the hydrogen split fraction in the stream H2 at the outlet of the ***SEP*** was fixed at 0.75 (Francesconi et al, 2007), whereas the split fractions of all the other components were taken as 0. The ***RSTOIC*** unit models the hydrogen oxidation reaction occurring in the fuel cell. The reactor specifics were completed by considering an operating temperature of 80°C and pressure of 1 atm; the inlet air at the cathode (AIR-FC), fed at 25°C and 1 atm, guarantees a 50% excess of oxygen in the ***RSTOIC*** reactor. In agreement with Ratnamala et al (2005), these conditions were considered as sufficient to assign total hydrogen conversion. The anode off-gas is sent to a burner, modeled as an adiabatic ***RSTOIC***, working at atmospheric pressure with 50% excess air (AIR-B); the complete combustion of all fuels contained (i.e. hydrogen, methane, carbon monoxide) was always imposed.
The heat required by the SR reactor working at temperature T_{SR} is supplied by the heat exchanger H-B, where the stream coming from the burner is cooled to T_{SR} +10°C. Model library ***HEATER*** was used for this purpose. An additional stream of fuel (CH4-B) is sent to the burner to satisfy the global heat demand of the system, when needed. The heat removed for cooling the stream at the outlet of heat exchanger H-B, at the inlet of HTS, LTS and PROX reactors and PEM fuel cell, as well as the heat for keeping the PROX at constant temperature, is employed to preheat the SR inlet stream. On the other hand, the heat removed for cooling the PEM fuel cell, is not recovered, since most of the times a simple air fan is used to cool the stack.
As concerns the flow sheet of a conventional ATR-based fuel processor (FP.B) coupled with a PEM fuel cell, for the sake of simplicity, the description of the flow sheet will be carried out by indicating the differences with respect to the flow sheet of Fig. 4, which are concentrated only in the reforming section. Indeed, in FP.B the reforming section is constituted by an adiabatic reactor (ATR), modeled by using model library ***RGIBBS***. The heat exchanger H-B can be suppressed in this configuration, since the ATR reactor has no heat requirement. The inlet temperature to the ATR reactor is fixed at 350°C, and is regulated by means of the heat exchanger H-ATR.

3.2 Innovative fuel processor – PEMFC systems

The integrated membrane-reactors were simulated by discretizing the membrane reactor with a series of N reactor-separator units. With this approximation, reactors are assumed to reach equilibrium and the separators are modeled as ideal separators, ***SEP***, whose output is

given by a stream of pure hydrogen (permeate) and a stream containing the unseparated hydrogen and all the balance (retentate). The amount of hydrogen separated ($n^i_{H2,P}$) is calculated assuming equilibrium between the partial pressure in the retentate and permeate side, according to Eq.2:

$$P_R \cdot \frac{n^i_{H2,R} - n^i_{H2,P}}{n_{R,i} + n^i_{H2,P}} = P^i_{H2,P} \tag{2}$$

where P_R is the pressure in the retentate side of the membrane, equals to reactor pressure; $n^i_{H2,R}$ is the mole flow of hydrogen in the retentate stream; n^i_R is the total mole flow of the retentate stream; $P^i_{H2,P}$ is hydrogen partial pressure in the permeate side of the membrane, calculated as:

$$P^i_{H2,P} = \frac{n^i_{H2,P}}{n^i_{H2,P} + n_{SG}} \cdot P_P \tag{3}$$

where P_P is the pressure in the permeate side of the membrane, taken as 1 atm in all the simulations, and n_{SG} represents the molar flow rate of steam sweep gas (SG), which can be introduced to increase the separation driving force in the membrane. When present, the sweep gas is produced by liquid water, fed at 25°C and 1 atm to a heat exchanger and sent to the membrane reactor in countercurrent flow mode.

The high hydrogen purity of the stream sent to the PEMFC allows taking as zero the anode off-gas, simplifying the model of the PEMFC to the cathode side (***RSTOIC***) only.

Fig. 5 reports the flow sheet used to simulate a membrane-SR reactor (FP.C) and a membrane-ATR reactor (FP.D) coupled with a PEMFC. The membrane-SR reactor was discretized with 30 units, whereas the membrane-ATR reactor was discretized with 20 units; the number of units required to model each membrane-reactor was assessed by repeating the simulations with an increasing number of reactor-separator units and was chosen as the minimum value above which global efficiency remained constant within ± 0.1%.

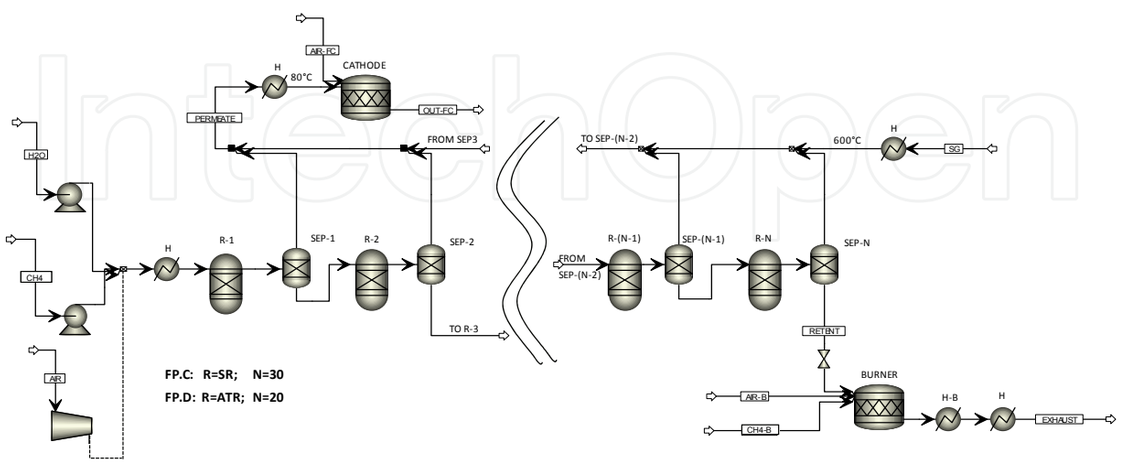

Fig. 5. Flowsheet of fuel processors FP.C and FP.D coupled with a PEMFC

As for the case of the conventional system, the heat eventually required by the reforming reactor is supplied by the heat exchanger H-B and an additional stream of fuel (CH4-B) is sent to the burner to satisfy the global heat demand of the system, when needed. The heat removed for cooling the streams at the outlet of heat exchanger H-B and at the inlet of the PEMFC is recovered to preheat SR inlet stream and eventually to produce sweep gas.
Fig. 6 reports the flow sheet used to simulate a SR-based FP coupled with a PEMFC, where the SR reactor is followed by a membrane WGS reactor (FP.E) and a ATR-based FP coupled with a PEMFC, where the ATR reactor is followed by a membrane WGS reactor (FP.F). With respect to FP.A and FP.B, in this case only one Water Gas Shift reactor is present, with an inlet temperature of 300°C; the membrane WGS reactor was discredited into four units.
As for the case of described above, the heat eventually required by the reforming reactor is supplied by H-B and an additional stream of fuel (CH4-B) is sent to the burner to satisfy the global heat demand of the system, when needed. The heat removed for cooling the streams at the outlet of heat exchanger H-B and at the inlet of the PEM fuel cell is recovered to preheat SR inlet stream and eventually to produce sweep gas.

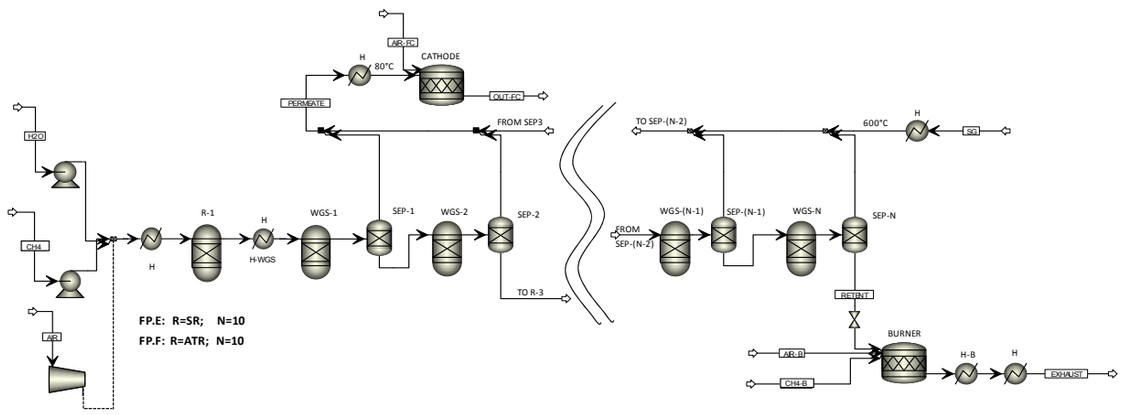

Fig. 6. Flow sheet of fuel processor FP.E and FP.F coupled with a PEMFC

All the reactors were considered as operating at the same pressure.
Auxiliary power units for compression of the reactants were considered in the configurations where pressure was explored as an operation variable, i.e. FP.C and FP.D.
100°C was chosen as the minimum exhaust gas temperature (T_{ex}), when compatible with the constraint of a positive driving force in the heat exchangers present in the plant.
Finally, it is worth mentioning that the assumptions made to model the system are the same for all the configurations investigated and do not affect the conclusions drawn in this comparative analysis.

3.3 System Efficiency

Energy efficiency, η, was defined according to the following Eq.4:

$$\eta = \frac{P_e - P_a}{(n_{CH4,F} + n_{CH4,B}) \cdot LHV_{CH4}} \tag{4}$$

where P_a is the electric power required by the auxiliary units for compression of methane, air and water, $n_{CH4,F}$ is the inlet molar flow rate of methane to the reactor, $n_{CH4,B}$ is the molar flow rate of methane fed to the burner, LHV_{CH4} is the lower heating value of methane and P_e is the electric power generated by the fuel cell, calculated as:

$$P_e = n_{H2} \cdot LHV_{H2} \cdot \eta_{FC} \tag{5}$$

where n_{H2} is the molar flow rate of hydrogen that reacts in the fuel cell, LHV_{H2} is the lower heating value of hydrogen, η_{FC} is the electrochemical efficiency of the cell, taken as 0.6 (Hou et al, 2007). In the membrane-based fuel cell systems, an important parameter is the global hydrogen recovery (HR), defined as:

$$HR = \frac{\sum_{i=1}^{N} n_{H2,P}^{i}}{n_{H2,R} + \sum_{i=1}^{N} n_{H2,P}^{i}} \tag{6}$$

where $n^{i}_{H2,P}$ is the molar flow rate of hydrogen separated by the i-th membrane unit, $n_{H2,R}$ is the molar flow rate of hydrogen in the RETENT stream at the exit of the last separator and N is the number of separators.
According to the definitions given above, η can be expressed as it follows:

$$\eta = (HR \cdot \eta_R \cdot \eta_{FC} - f_a) \cdot (1 - \alpha) \tag{7}$$

where f_a is the fraction of inlet methane required to run the auxiliary units, defined by Eq. 8:

$$f_a = \frac{P_a}{n_{CH4,F} \cdot LHV_{CH4}} \tag{8}$$

α is the ratio between methane flow rate fed to the burner and total methane flow rate fed to the system, defined by Eq. 9:

$$\alpha = \frac{n_{CH4,B}}{n_{CH4,F} + n_{CH4,B}} \tag{9}$$

f_R is the reforming factor, defined by Eq. 10:

$$f_R = \frac{\left(n_{H2,R} + \sum_{i=1}^{N} n_{H2,P}^{i} \right) \cdot LHV_{H2}}{n_{CH4,F} \cdot LHV_{CH4}} \tag{10}$$

This factor is related to the global amount of hydrogen produced in the fuel processor per moles of methane fed to the reforming reactor; therefore it does not depend on the heat requirement of the system.

4. Results

Simulation where performed by varying the main operating parameters for each system. The parameters investigated and the ranges explored are reported in Table 1. For conventional systems (FP.A and FP.B) pressure was fixed at 1 atm since reforming processes are inhibited by pressure increase, whereas the WGS and PROX processes are independent of pressure. The operating ranges of H_2O/CH_4 and T_{SR} for the system with membrane SR reactor (FP.C) are chosen in order to guarantee thermal stability of the membrane and to avoid coke formation. The pressure range investigated for the innovative systems was chosen in order to guarantee the mechanical resistance of the membrane. The operating ranges of H_2O/CH_4 and of O_2/CH_4 for the ATR systems are chosen in order to avoid coke formation and to guarantee the autothermicity of the process (Seo et al, 2002).

	Case	H_2O/CH_4	O_2/CH_4	T_{SR} [°C]	SG/CH_4	P [atm]
SR	FP.A	2.0 – 6.0	-	600 - 800	-	1
	FP.C	2.5 – 6.0	-	500 - 600	0 – 3.0	3 - 15
	FP.E	2.0 – 6.0	-	600 - 800	0 – 3.0	3 - 15
ATR	FP.B	1.2 – 4.0	0.3 – 1.0	-	-	1
	FP.D	1.2 – 4.0	0.3 – 1.0	-	0 – 3.0	3 - 15
	FP.F	1.2 – 4.0	0.3 – 1.0	-	0 – 3.0	3 - 15

Table 1. Range of operating parameters investigated

4.1 Conventional Fuel Processors

Fig. 7 shows the trend of energy efficiency η, methane conversion x_{CH4}, reforming factor f_R and the fraction of total inlet methane that is sent to the burner α as a function of H_2O/CH_4, parametric in the steam reforming reactor temperature.

For all the temperatures investigated, an increase of water content in the feed has a positive effect on methane conversion x_{CH4} and on the reforming factor f_R. This well note trend is due to the fact that water is a reactant of reforming reactions.

For each temperature and until a certain value of H_2O/CH_4, the value of α is equal to zero. For higher H_2O/CH_4, the increase of this ratio leads to an increase of α; indeed, the increase of H_2O/CH_4 causes an increase of the heat required to sustain the reforming process, moreover the improvement of reforming reactor performance with H_2O/CH_4 causes a reduction of the heating value of the AOG stream, thus an increase of the quantity of methane that needs to be sent to the burner for sustaining the endothermicity of the process.

As described in the System efficiency Section, the energy efficiency is a combination of f_R and of α; indeed, η shows a non monotone trend as a function of H_2O/CH_4 because, although an increase of water content causes a continuous increase of reforming reactor performance, the amount of methane sent to the burner also increases with H_2O/CH_4.

For all the H_2O/CH_4 investigated, the increase of reforming reactor temperature (T_{SR}) causes an increase of x_{CH4}, f_R and α. Energy efficiency η shows a different trend on the basis of the

weight of these factors: for low H_2O/CH_4, η shows a continuous increase with T_{SR} in the range investigated, whereas, for high H_2O/CH_4, η shows a non monotone trend with T_{SR}.

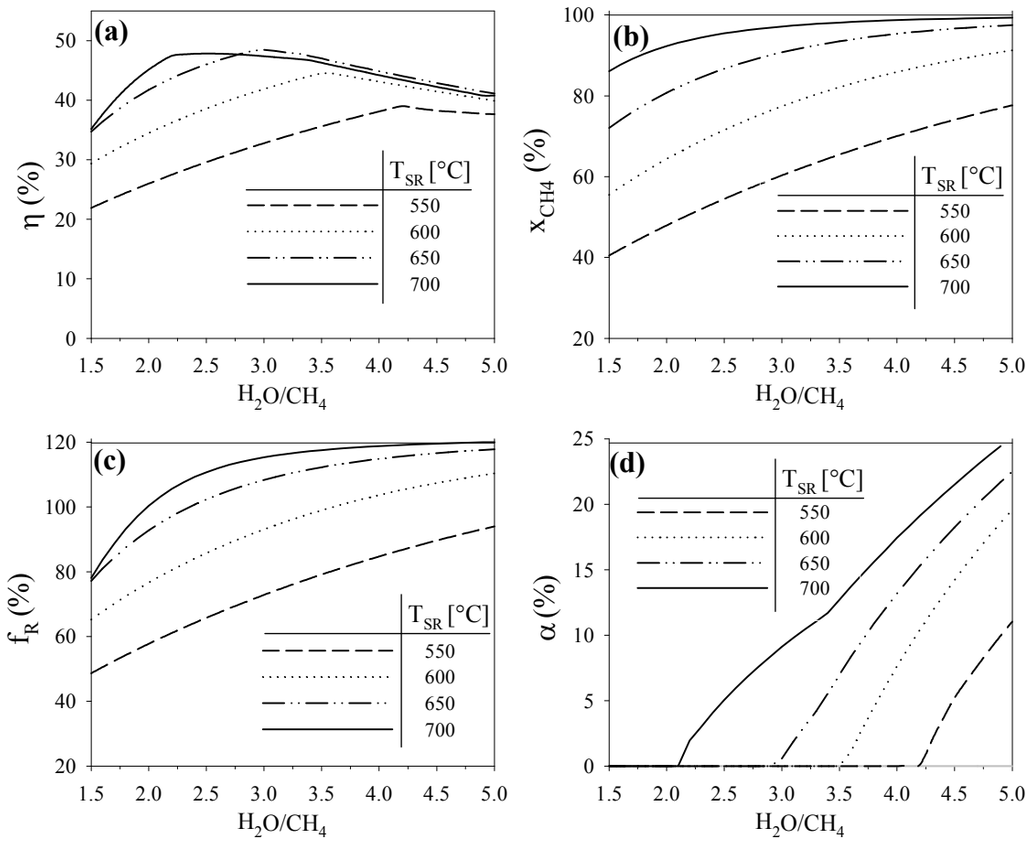

Fig. 7. η (a), x_{CH4} (b), f_R (c) and α (d) as a function of H_2O/CH_4 parametric in T_{SR}

Fig. 8 shows the trend of energy efficiency η, methane conversion x_{CH4}, reforming factor f_R for conventional ATR-based fuel processor – PEMFC systems (systems with FP.B), as a function of O_2/CH_4 parametric in H_2O/CH_4.

Methane conversion shows a monotone increase as a function of O_2/CH_4. The effect of water addition on methane conversion is positive in case x_{CH4} is far lower than unity, whereas this effect can be considered as negligible when the conversion approaches to unity. Reforming factor shows a non monotone trend as a function of O_2/CH_4; indeed, for low O_2/CH_4 values the process cannot reach the temperature values that favor the reforming reactions, whereas for high O_2/CH_4 values, although the reforming temperature results to be strongly increased, the hydrogen and methane oxidation reactions are favorite, with subsequent reduction of the amount of hydrogen produced and, thus, of the f_R.

The addition of water leads to an increase of f_R, being water a reactant of the reforming reactions; this increase becomes negligible for H_2O/CH_4 values higher than 2.

For all the O_2/CH_4 and H_2O/CH_4 values investigated, α remains equal to zero, therefore, the trend of energy efficiency results to be the same of the reforming factor; moreover, there is a waste of heat from the system, related to the autothermic nature of the process, which hinders the possibility of recovering the energy content of the AOG.

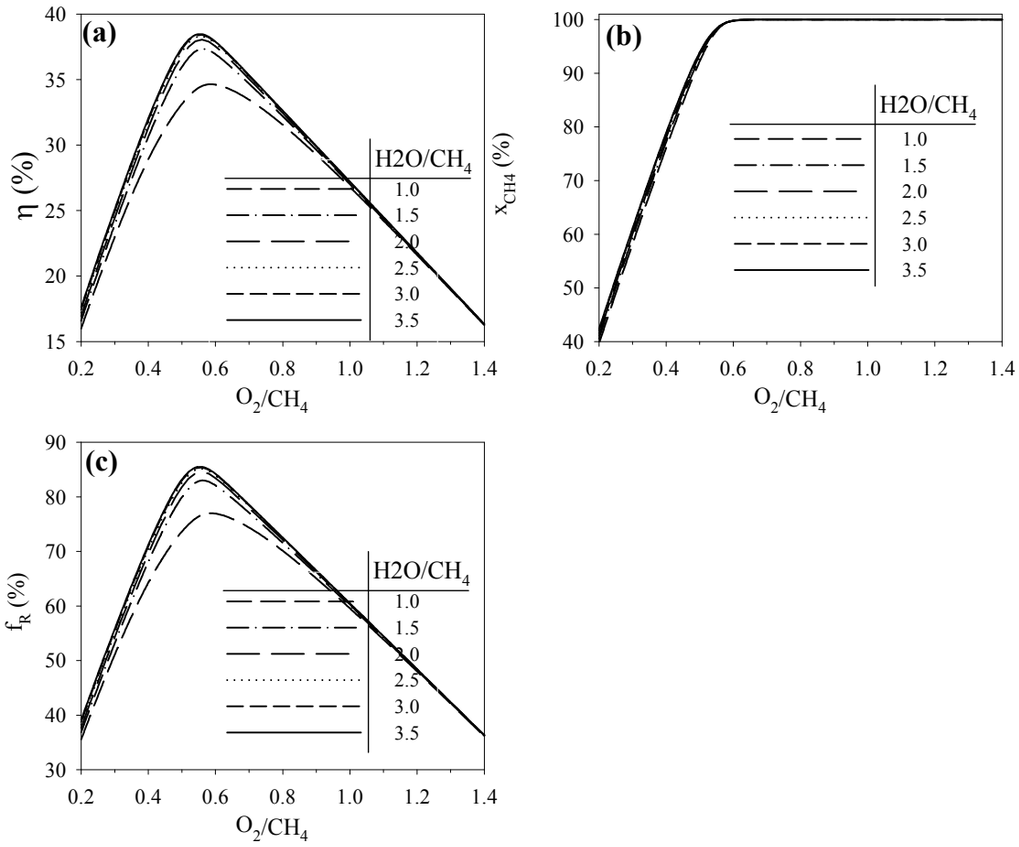

Fig. 8. η (a), x_{CH4} (b) and f_R (c) as a function of O_2/CH_4 parametric in H_2O/CH_4.

Table 2 reports the simulation results and the value of the operative parameters given as simulation input that maximize the energy efficiency η, for FP.A and for FP.B, respectively. FP.A shows the highest global efficiency (48.0%) at T_{SR}=670°C and H_2O/CH_4=2.5. It should be noticed that, in the optimal conditions, methane conversion (x_{CH4}) is lower than unity; however, the non converted methane is not energetically wasted, since it contributes to the energy content of the AOG, used to sustain the endothermicity of the SR reactor. In this conditions, no addition of methane to the burner is needed (α=0). According to the flow sheet of FP.A, the minimum exhaust gas temperature achievable is 226°C. Further heat recovery is hindered by temperature cross-over in the heat exchangers.

Simulation results				
	x_{CH4}	**α**	**η**	**T_{EX} (°C)**
FP.A (SR)	91.0	0.0	48.0	226
FP.B (ATR)	98.8	0.0	38.5	444
Simulation Input				
	P (atm)	**H_2O/CH_4**	**O_2/CH_4**	**T_{SR} (°C)**
FP.A (SR)	1	2.5	-	670
FP.B (ATR)	1	4.0	0.56	-

Table 2. Conventional Fuel Processor – PEMFC systems

FP.B shows the highest global efficiency (38.5%) at O_2/CH_4=0.56 and H_2O/CH_4=4.0; the value of η is significantly lower than what achieved with FP.A, mainly due to the autothermal nature of the ATR process, that limits the possibility to recover the energy content of the AOG. This reflects into a higher exhaust gas temperature in FP.B (444°C) than in FP.A (226°C).

4.2 Innovative Fuel Processors

Fuel Processors based on membrane reforming reactor

Fig. 9 reports the energy efficiency of system with FP.C as a function of pressure.
Energy efficiency rapidly increases with pressure in the range 3-5 atm, where no methane addition to the burner is required to sustain the endothermic steam reforming reaction.

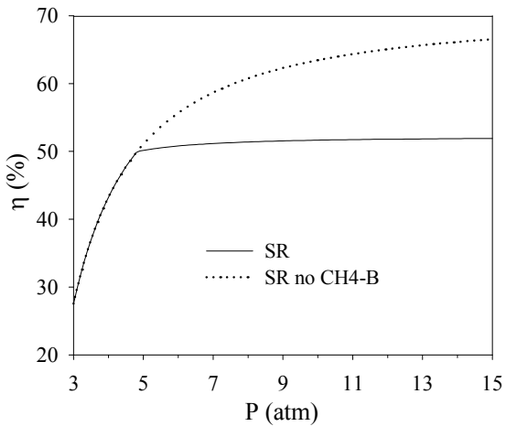

Fig. 9. η as a function of pressure for system with FP.C. Operating conditions: T_{SR}=600°C, H_2O/CH_4=2.5, SG/CH_4=0

As pressure increases above 5 atm ca, η continues to grows with pressure, but at a lower rate, because methane addition to the burner becomes necessary. The dotted line, superimposed to Fig. 9 as an aid to this discussion, represents the value of η that would be calculated if the methane sent to the burner was not factored in the computation.
The trend of η vs P is the combined effect of hydrogen recovery (HR), reforming factor (f_R), the power of the auxiliary units (related to f_a), whose values are reported in Table 3 together with the value of methane conversion (x_{CH4}) and fraction of methane sent to the burner (α).

P (atm)	x_{CH4}	α	T_{EX} (°C)	HR	fa	f_R	η
3	70.6	0	803.8	58	0.5	80.4	27.5
5	86.3	1.8	100	85.9	0.7	100.5	50.2
7	91.8	12.8	100	91.9	0.9	108.0	51.2
9	94.5	17.2	100	94.4	1.1	111.8	51.5
12	96.6	20.4	100	96.2	1.3	114.9	51.8
15	97.6	22	100	97.1	1.4	116.7	51.9

Table 3. System with FP.C. Operating conditions: T_{SR}=600°C, H_2O/CH_4=2.5, SG/CH_4=0

In particular, HR increases with pressure due to the increase of hydrogen separation driving force through the membrane; f_R increases with pressure because it is positively influenced by the trend of HR with pressure, due to the positive effect on reaction equilibrium of increasing hydrogen separation. f_a increases with pressure, due to increasing compression ratios. To complete the picture, it should be kept in mind that the heating value of the retentate decreases with pressure, as a consequence of higher x_{CH4} and HR. This, in turn, influences the quantity of methane sent to the burner to sustain the endothermic steam reforming reaction.
In the low pressure range, the positive effect of HR and f_R on energy efficiency overrules the negative effect of f_a and α. The plateau value reached at higher pressure indicates that the drawback of f_a and α compensates the positive effect of HR and f_R.
Fig. 10 reports the effects of SG/CH_4 on system efficiency of FP.C parametric in pressure, at a fixed outlet exhaust gases temperature of 100°C. Simulation details for P = 10 atm are reported in Table 4.

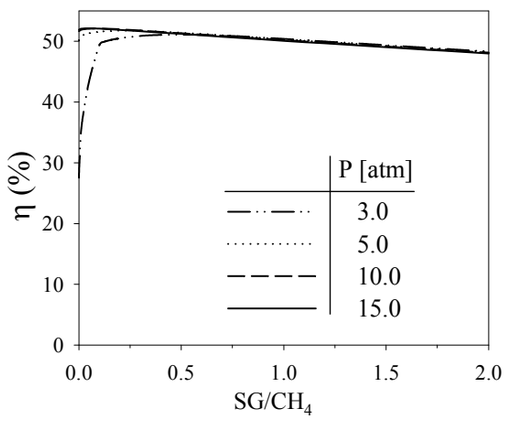

Fig. 10. η as a function of SG/CH_4 parametric in pressure for system with FP.C. Operating conditions: T_{SR}=600°C, H_2O/CH_4=2.5

SG/CH4	x_{CH4}	α	T_{EX} (°C)	HR	fa	f_R	η
0.0	95.4	18.6	100.0	95.1	1.1	113.1	51.6
0.1	99.8	25.7	100.0	99.1	1.1	119.8	52.1
0.5	100.0	28.5	100.0	100.0	1.1	121.4	51.3
1.0	100.0	30.0	100.0	100.0	1.1	121.3	50.2
1.5	100.0	31.5	100.0	100.0	1.2	121.3	49.1
2.0	100.0	33.0	100.0	100.0	1.2	121.5	48.1

Table 4. System with FP.C. Operating conditions: T_{SR}=600°C, H_2O/CH_4=2.5, P=10 atm

It is possible to observe that η shows a maximum as a function of SG/CH_4 ratio, which shifts leftwards and upwards as pressure increases. For each pressure value investigated, hydrogen recovery is enhanced by the presence of the sweep gas, as a consequence of reduced hydrogen partial pressure in the permeate side; this leads also to an increase of f_R thanks to the positive effect of hydrogen removal on reactions equilibrium.
However, the production of sweep gas is always coupled with addition of methane to the burner, with an increment of α that can overrule the increment of HR and f_R. For this reason,

being η combination of f_R, HR and α, after an initial small increment, it decreases with addition of sweep gas.
The effect of pressure depends on the SG/CH_4 value. For low SG/CH_4, an increase of pressure causes an increase of η, whereas a decreasing trend of the η with pressure is observed at high SG/CH_4. This is due to the fact that the increment of pressure increases both HR and f_a; when SG/CH_4 is high, HR becomes close to 100% already at low pressure values, therefore an increase of pressure only causes an increase of f_a, lowering η.
Table 5 report the detail of the simulation results and value of the operating parameters given as simulation input that maximize the energy efficiency η, for FP.C.
The best way to operate a membrane SR system is to increase the pressure without addition of sweep gas.
It is possible to observe that the energy efficiency of a SR-based system is increased if a membrane reactor is used (FP.C), in place of a conventional reactor. This is due to the possibility to recover a higher amount of heat in FP.C than in FP.A. Indeed the heat exchanger network needed in FP.A has to satisfy the temperature requirements of the Shift and PROX reactors resulting in a higher exhaust gas temperature (226°C), while in FP.C the heat exchanger network allows to cool the exhaust gas to 100°C (as chosen in the methodology), without any temperature cross over.

Simulation results						
	f_R	**α**	**HR**	**f_a**	**η**	**T_{EX} (°C)**
FP.C (SR)	120.0	25.6	99.2	1.3	52.2	100.0
Simulation Input						
		P (atm)	**H_2O/CH_4**	**T_{SR} (°C)**	**SG/CH_4**	
FP.C (SR)		15	2.5	600	0.1	

Table 5. Membrane SR – PEMFC system based on membrane reforming reactor

Fig. 11 reports energy efficiency of system with FP.D as a function of pressure. As for the case of FP.C, η shows a continuous increase with pressure, but the values are significantly lower, due to limited recovery of the energy contained in the retentate stream and to the negative contribution of the compressor (see T_{ex} and f_a in Table 6).

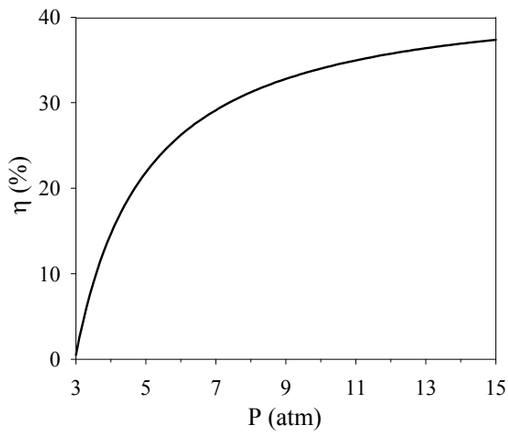

Fig. 11. η as a function of pressure for system with FP.D. Operating conditions: O_2/CH_4=0.48, H_2O/CH_4=1.15, SG/CH_4=0

It should be noted that, in FP.D, the maximum value of η (37.2%) is even lower than what is obtained with the conventional ATR reactor (η = 38.5%). This should be attributed to the fact that, notwithstanding the absence of the AOG stream, the dilution of the reacting mixture with nitrogen reduces HR (affecting, in turn, also x_{CH4}) leading to a retentate with relatively high amount of methane and hydrogen, whose heating value cannot be totally recovered.
It should be pointed out that, due to the exothermic nature of the reactions, no additional methane to the burner is required, i.e. α=0, and the exhaust gas stream leaves the plant at quite high temperatures. Data are reported in Table 6.

P (atm)	x_{CH4}	α	T_{EX} (°C)	HR	fa	f_R	η
3.0	85.2	0.0	1369.1	5.8	1.6	60.1	0.5
5.0	88.4	0.0	1248.1	60.2	2.6	67.6	21.8
7.0	90.0	0.0	1178.1	75.6	3.3	71.4	29.1
9.0	90.9	0.0	1132.7	82.7	3.9	73.8	32.7
12.0	91.8	0.0	1089.8	88.0	4.6	76.2	35.6
15.0	92.4	0.0	1063.6	90.9	5.2	77.8	37.2

Table 6. System with FP.C. Operating conditions: O_2/CH_4=0.48, H_2O/CH_4=1.15, SG/CH_4=0

Fig. 12 reports the energy efficiency of system with FP.D as a function of SG/CH_4 parametric in pressure. Simulation details for P = 10 atm are reported in Table 7.

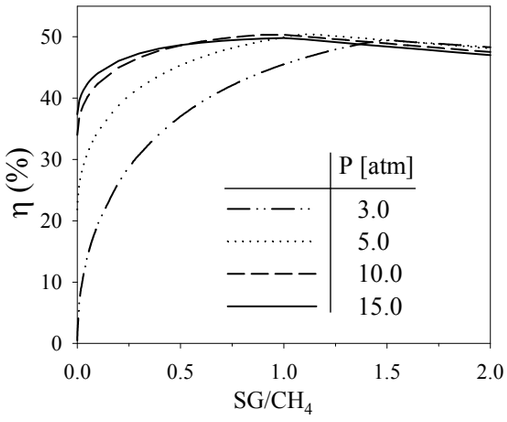

Fig. 12. η as a function SG/CH_4 parametric in pressure for system with FP.D. Operating conditions: O_2/CH_4=0.48, H_2O/CH_4=1.15

SG/CH_4	x_{CH4}	α	T_{EX} (°C)	HR	fa	f_R	η
0.0	91.3	0.0	1115.9	84.9	4.1	74.8	34.0
0.1	95.1	0.0	894.7	95	4.1	81.5	42.4
0.5	99.1	0.0	463.8	99.1	4.1	88.6	48.6
1.0	100	0.4	100.0	99.9	4.1	91.2	50.3
1.5	100	4.0	100.0	100.0	4.1	91.8	48.9
2.0	100	7.0	100.0	100.0	4.1	91.9	47.5

Table 7. System with FP.D. Operating conditions: O_2/CH_4=0.48, H_2O/CH_4=1.15, P=10 atm

The trend of η with SG/CH_4 and pressure is similar to the one observed for the system based on SR. However, it is important to note that for each pressure value investigated, the SG/CH_4 value that maximizes energy efficiency is higher than the corresponding one in the SR-based fuel processor.
This is due to the fact that in an ATR-based system, there is an excess energy due to the autothermic nature of the process, that allows a consistent sweep gas production without methane addition to the burner, i.e. α=0.
Moreover, it is worth noting that energy efficiency of FP.D is highly improved by adding sweep gas, increasing from 34.0% (SG/CH_4=0) to 50.3% (SG/CH_4=1.0).
Table 8 report the detail of the simulation results and value of the operating parameters given as simulation input that maximize the energy efficiency η, for FP.D.

Simulation results						
	f_R	**α**	**HR**	**f_a**	**η**	**T_{EX} (°C)**
FP.D	90.2	0.0	99.6	3.3	50.6	100.0
Simulation Input						
		P (atm)	**H_2O/CH_4**	**O_2/CH_4**	**SG/CH_4**	
FP.D (ATR)		7	1.2	0.5	1.0	

Table 8. Membrane ATR – PEMFC system based on membrane reforming reactor.

The best way to operate an autothermal reforming membrane system is to moderately increase pressure and to employ some sweep gas to improve HR (the maximum η is reached for P=7 atm and SG/CH_4=1.0, as reported in Table 7).
The lower value of pressure that maximize η with respect to SR system is due to the higher power required by the auxiliary units, needed essentially to compress the air in the feed.
Finally, it should be noted that the addition of sweep gas in system with FP.D allows reaching energy efficiency values significantly higher than the optimum value of the conventional system (38.5%) and similar to the energy efficiency of SR based systems.
It should be kept in mind that, due to limited thermal stability of the highly selective membranes, membrane units should not be exposed to temperatures higher than 600°C. While FP.C always meets this constraint (since reactor temperature is fixed at 600°C), FP. D does not. Indeed, in the optimal conditions, the first reactors reach temperatures as high as 720°C. Therefore, the actual realization of an integrated membrane reactor would require significant improvements of membrane compatibility with high temperatures. A more realistic configuration of an ATR based membrane reactor should consider a first ATR reactor, where most of the methane oxidation takes place, followed by a membrane reactor, interposing between the two units a heat exchanger to cool down the temperature before entrance into the membrane reactor, so that the membranes are never exposed to temperatures higher than 600°C. With this configuration, energy efficiency becomes 48.5% and the best operating conditions are P=7 atm; O_2/CH_4=0.5; H_2O/CH_4=1.7; SG/CH_4=1.0.

Fuel Processors based on membrane WGS reactor

Optimization performed for systems based on membrane WGS reactors (FP.E for SR and FP.F for ATR) followed the same criteria of what reported for systems based on membrane reforming reactors. Although quantitatively different, the trend of performance with operating parameters were similar to what reported for the systems with membrane reforming reactors, therefore data are not reported for the sake of brevity.

Table 9 reports the simulation results and the value of the operating parameters given as simulation input that maximize the energy efficiency η, for FP.E and for FP.F, respectively.
It is possible to observe that the introduction of the membrane in the WGS reactor allows obtaining higher energy efficiencies than what achieved in the conventional systems.

Simulation results						
	f_R	**A**	**HR**	**fa**	**η**	**T_{EX} (°C)**
FP.E (SR)	110.9	18.4	96.8	0.5	52.2	141.5
FP.F (ATR)	83.0	0.0	99.4	1.9	47.6	100.0
Simulation Input						
	P (atm)	**H_2O/CH_4**	**O_2/CH_4**	**SG/CH_4**	**T_{SR} (°C)**	**T_{WGS} (°C)**
FP.E (SR)	3	2.0	-	0.2	800	300
FP.F (ATR)	3	1.2	0.6	1.9	-	300

Table 9. Innovative Fuel Processor – PEMFC systems based on membrane WGS reactor

As far as system with FP.E is concerned, the temperature value required for system optimization corresponds to the highest value investigated; this is due to the positive effect of temperature on the SR reactor, and thus on the membrane WGS reactor, that overcomes the negative effect of temperature increase on α.
The maximum efficiency value is limited by the problem of a not complete heat recovery of the exhaust gases (T_{EX}>100°C); this is due to the problem of temperature cross-over that can arise in the heat exchangers when the system works at high SR temperatures.
Since the endothermic nature of the process imposes the necessity of operating with additional methane to the burner, the amount of sweep gas required to optimize the system is small (SG/CH_4=0.2).
It is also possible to observe that the pressure value required for system optimization corresponds to the lowest value investigated; this is due to the negative effect of pressure on the SR reactor, which overcomes the positive effect of pressure increase on the membrane WGS reactor. This one, indeed, allows reaching a high HR, notwithstanding the low pressure value, thanks to the high hydrogen concentration achieved at the outlet of the SR reactor, which positively acts on the driving force.
As far as system with FP.F is concerned, it is possible to observe that the value of H_2O/CH_4 that maximizes the energy efficiency is by far lower than what required for the conventional case. For the ATR systems, indeed, the autothermal nature of the process allows to have an excess heat in the system that can be used to produce steam. In the conventional system, the steam can be used only as reactant, with only moderate improvement of energy efficiency for H_2O/CH_4>3, thus making further steam production useless. In the innovative system, the steam can be used as reactant as well as sweep gas and the energy efficiency resulted to be favored more by an increase of SG/CH_4 than by an increase of H_2O/CH_4.
The autothermal nature of the process allows operating with no additional methane to the burner and the high amount of sweep gas allows the system to operate at low pressure values, favoring the conditions in the ATR reactor.
Although working at the same pressure, the fraction of inlet methane required to run the auxiliary unit is higher in the ATR case than in the SR case, for the presence of air in the feed (f_a=0.5 for FP.E and 1.9 for FP.F).
It is also possible to note that the introduction of the membrane in the WGS reactor not only allows to reach efficiency values higher than what achieved in the conventional systems, but

also makes the SR and ATR based systems similar in terms of energy efficiency (the difference between SR and ATR in the conventional case is ca. 20%, whereas in this case it is only ca. 8%).

5. Conclusions

As a general conclusion on system analysis, the optimum of each fuel processor – PEMFC system and the corresponding operating parameters are reported in Table 9.
It is possible to observe that the SR-based processes always show higher energy efficiency than the corresponding ATR-based processes, with a marked difference in the case of conventional systems (FP.A and FP.B have a difference of about 21% in the energy efficiency value). However, the introduction of the membrane allows to obtain energy efficiency values of the ATR system closer to the efficiency levels reached in the SR ones (differences between SR and ATR based systems of ca. 7% when the membrane is introduced in the reforming reactor and of ca. 9% when the membrane is introduced in the WGS reactor).

	Case	H_2O/CH_4	O_2/CH_4	T_{SR} [°C]	SG/CH_4	P [atm]	η %
SR	FP.A	2.5	-	670	-	1	48.0
	FP.C	2.5	-	600	0.1	15	52.1
	FP.E	2.0	-	800	0.2	3	52.2
ATR	FP.B	4.0	0.56	-	-	1	38.5
	FP.D	1.7	0.5	-	1.0	7	48.5
	FP.F	1.2	0.6	-	1.9	3	47.6

Table 10. Comparison of various FP – PEMFC systems in correspondence of operating conditions that maximize system performance

The comparison between the steam reforming based systems (innovative systems with FP.C and FP.E vs conventional system with FP.A) showed that the employment of a membrane reactor can increase system efficiency from 48.0% to values above 52.0%. Such an efficiency increase requires almost no addition of sweep gas due to the endothermic nature of the process.
The pressure that optimizes the energy efficiency of the two membrane-based system is different; the system with integrated reforming reactor (FP.C) requires to operate at high pressure value (15 atm), whereas the system with membrane WGS reactor (FP.E) at low pressure value (3 atm). This is due to the fact that the SR reactor is negatively influenced by the pressure increase; therefore the system is optimized by increasing the hydrogen recovery in the membrane WGS reactor by increasing hydrogen concentration at the inlet of the WGS reactor more than by increasing pressure.
As regards temperature, all systems require to operate at the highest possible temperature compatible with material stability.
However, although the limit on temperature imposed to the system with membrane reforming reactor is more tighten, energy efficiency results to be as high as the value reached in the system with membrane WGS reactor, that operates at high SR temperature. This is due to the fact than the hydrogen removal from the reaction environment allows to achieve higher performance at lower temperature.
The comparison between the autothermal reforming systems (innovative systems with FP.D and FP.F vs conventional system FP.B) shows that energy efficiency can be improved from

38.5% to values around 48%, if a membrane reactor is employed. To obtain such an energy efficiency improvement, sweep gas addition is required.
The considerations on pressure are the same of what reported for the SR case, although the system with membrane reforming reactor is optimized at pressure values lower that the SR case (7 atm instead of 15 atm) due to the higher value of power required to run the auxiliary units.
It is possible to observe that the value of H_2O/CH_4 that maximizes the energy efficiency of the innovative ATR systems is far lower than what required for the conventional case.
Indeed, in the innovative systems, the steam can be used as reactant and as sweep gas and the energy efficiency resulted to be favored more by an increase of SG/CH_4 than by an increase of H_2O/CH_4.

6. References

Ahmed, S. Krumpelt, M. (2001). Hydrogen from hydrocarbon fuels for fuel cells, *International Journal of Hydrogen Energy,* 26, 291–230, ISSN 0360-3199

Aspen Technology Inc. http://www.aspentech.com

Basile, A. Chiappetta, G. Tosti, S. Violante, V. (2001). Experimental and simulation of both Pd and Pd/Ag for a water gas shift membrane reactor, *Separation and purification technology,* 25, 549-571, ISSN 1383-5866

Campanari, S. Macchi, E. Manzolini, G. (2008). Innovative membrane reformer for hydrogen production applied to PEM micro-cogeneration: Simulation model and thermodynamic analysis, *International Journal of Hydrogen Energy,* 33, 1361-1373, ISSN 0360-3199

Ersoz, A. Olgun, H. Ozdogan, S. (2006). Reforming options for hydrogen production from fossil fuels for PEM fuel cells, *Journal of Power Sources,* 154, 67-73, ISSN 0378-7753

Francesconi, JA. Mussati, MC. Mato, RO. Aguirre, PA. (2007). Analysis of the Energy efficiency of a integrated ethanol processor for PEM fuel cell systems, *Journal of Power Sources,* 167, 151–161, ISSN 0378-7753

Hou, J. Zhuang, M. Wag, G. (2007). The analysis for the efficiency properties of the fuel cell engine, *Renewable Energy,* 32, 1175-1186, ISSN 0960-1481

Larminie, J. & Dicks, A. (2004). *Fuel Cell Systems Explained, Second Edition,* John Wiley & Sons Ltd, 0-470-84857-X, The Atrium, Southern Gate, Chichester, West Sussex PO19 8SQ, England

Lampert, J. (2004). Selective catalytic oxidation: a new catalytic approach to the desulfurization of natural gas and liquid petroleum gas for fuel cell reformer applications, Journal of Power Sorces, 131, 27-34, ISSN 0378-7753

Lattner, R. Harold, MP. (2004). Comparison of methanol-based fuel processors for PEM fuel cell systems. *International Journal of Hydrogen Energy,* 29, 393-417, ISSN 0360-3199

Lattner, R. Harold, MP. (2005). Comparison of conventional and membrane reactor fuel processors for hydrocarbon-based PEM fuel cell systems, *Applied Catalysis B: Environmental,* 56, 149-169, ISSN 0926-3373

Lyubovsky, M. Walsh, D. (2006). Reforming system for co-generation of hydrogen and mechanical work, *Journal of Power Sources,* 157, 430–437, ISSN 0378-7753

Manzolini, G. Tosti, S. (2008). Hydrogen production from ethanol steam reforming: energy efficiency analysis of traditional and membrane processes, *International Journal of Hydrogen Energy,* 33, 5571-5582, ISSN 0360-3199

Pearlman, B. Bhargav, A. Shields, EB. Jackson, GS. Hearn, PL. (2008). Modeling efficiency and water balance in PEM fuel cell systems with liquid fuel processing and hydrogen membranes, *Journal of Power Sources,* 185, 1056–1065, ISSN 0378-7753

Ratnamala, GM. Shah, N. Mehta, V. Rao, PV. (2005). Integrated Fuel Cell Processor for a 5-kW Proton-Exchange Membrane Fuel Cell, *Industrial & Engineering Chemistry Research,* 44, 1535-1541, ISSN 0888-5885

Semelsberger, TA. Brown, LF. Borup, RL. Inbody, MA. (2004). Equilibrium products from autothermal processes for generating hydrogen-rich fuel-cell feeds, *International Journal of Hydrogen Energy,* 29, 1047-1064, ISSN 0360-3199

Seo, YS. Shirley, A. Kolaczkowski, ST. (2002). Evaluation of thermodynamically favourable operating conditions for production of hydrogen in three different reforming technologies, *Journal of Power Sources,* 108, 213–225, ISSN 0378-7753

Shu, J. Grandjean, BPA. van Neste, A. Kaliaguine, S. (1991). Catalytic palladium-based membrane reactors: a review, *Canadian Journal of Chemical Engineering*, 69, 1036-1060, ISSN 0008-4034

Song, C. (2002). Fuel processing for low-temperature and high-temperature fuel cells: Challenges, and opportunities for sustainable development in the 21st century, *Catalysis Today,* 77, 17–49, ISSN 0920-5861

Xu, J. Froment, GF. (1989). Methane Steam Reforming, Methanation and Water-Gas Shift. Intrinsic Kinetics, *AIChE Journal,* 35, 88-96, ISSN 0001-1541

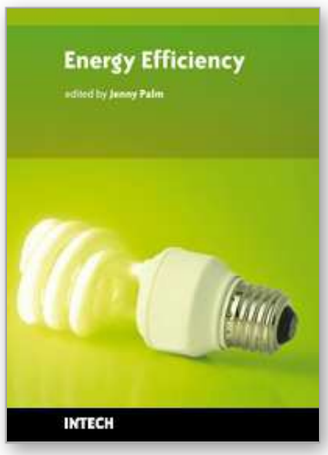

Energy Efficiency
Edited by Jenny Palm

ISBN 978-953-307-137-4
Hard cover, 180 pages
Publisher Sciyo
Published online 17, August, 2010
Published in print edition August, 2010

Global warming resulting from the use of fossil fuels is threatening the environment and energy efficiency is one of the most important ways to reduce this threat. Industry, transport and buildings are all high energy-using sectors in the world and even in the most technologically optimistic perspectives energy use is projected to increase in the next 50 years. How and when energy is used determines society's ability to create long-term sustainable energy systems. This is why this book, focusing on energy efficiency in these sectors and from different perspectives, is sharp and also important for keeping a well-founded discussion on the subject.

How to reference
In order to correctly reference this scholarly work, feel free to copy and paste the following:

Marino Simeone, Lucia Salemme and Laura Menna (2010). Analysis of the Energy Efficiency of Fuel Processor - PEM Fuel Cell Systems, Energy Efficiency, Jenny Palm (Ed.), ISBN: 978-953-307-137-4, InTech, Available from: http://www.intechopen.com/books/energy-efficiency/analysis-of-the-energy-efficiency-of-fuel-processor-pem-fuel-cell-systems

INTECH
open science | open minds

InTech Europe
University Campus STeP Ri
Slavka Krautzeka 83/A
51000 Rijeka, Croatia
Phone: +385 (51) 770 447
Fax: +385 (51) 686 166
www.intechopen.com

InTech China
Unit 405, Office Block, Hotel Equatorial Shanghai
No.65, Yan An Road (West), Shanghai, 200040, China
中国上海市延安西路65号上海国际贵都大饭店办公楼405单元
Phone: +86-21-62489820
Fax: +86-21-62489821

IntechOpen